Variable domain-linked oligosaccharides of a human monoclonal IgG: structure and influence on antigen binding

Haike LEIBIGER[1], Daniel WÜSTNER, Rolf-Dietrich STIGLER and Uwe MARX[2]

Department of Medical Immunology, Medical School (Charité), Humboldt-University, Tucholskystr. 2, D-10117 Berlin, Germany

The variable-domain-attached oligosaccharide side chains of a human IgG produced by a human–human–mouse heterohybridoma were analysed. In addition to the conserved N-glycosylation site at Asn-297, an N-glycosylation consensus sequence (Asn-Asn-Ser) is located at position 75 in the variable region of its heavy chain. The antibody was cleaved into its antigen-binding (Fab) and crystallizing fragments. The oligosaccharides of the Fab fragment were released by digestion with various *endo*- and *exo*glycosidases and analysed by anion-exchange chromatography and fluorophore-assisted carbohydrate electrophoresis. The predominant components were disialyl- bi-antennary and tetra-sialyl tetra-antennary complex carbohydrates. Of note is the presence in this human IgG of oligosaccharides containing *N*-glycolylneuraminic acid and *N*-acetylneuraminic acid in the ratio of 94:6. Furthermore, we determined *N*-acetylgalactosamine in the Fab fragment of this antibody, suggesting the presence of O-linked carbohydrates. A three-dimensional structure of the glycosylated variable (Fv) fragment was suggested using computer-assisted modelling. In addition, the influence of the Fv-associated oligosaccharides of the CBGA1 antibody on antigen binding was tested in several ELISA systems. Deglycosylation resulted in a decreased antigen-binding activity.

Key words: antibody, carbohydrate, CHARMm, energy minimization, fluorophore-assisted carbohydrate electrophoresis.

INTRODUCTION

Antibodies are glycoproteins containing 3–12 % carbohydrates at conserved N-glycosylation sites located in the constant regions of their heavy chains. Glycosylation of these sites seems to have little, if any, effect on antigen binding [1]. Some antibodies have also been reported with N-glycosylation sites in the variable regions [2,3]. Approximately 15–25 % of the antigen-binding (Fab) fragments and 15 % of the light chains isolated from human myeloma proteins contain N-linked oligosaccharides [4]. Since neither kappa nor lambda constant regions contain potential N-linked carbohydrate consensus sequences, the light-chain-linked oligosaccharides are presumed to be present on the variable regions [5,6].

The presence of large, bulky carbohydrates on the surfaces of the variable regions of an immunoglobulin contributes to, and probably alters, the conformation of the protein at this site. Therefore, glycosylation in the variable domains often seems to interfere with the antigen-binding properties of these antibodies [2,7,8]. There is limited information concerning the structures of Fab-linked oligosaccharides. The N-linked carbohydrate structures found in the variable regions seem to differ from those present in the constant region of IgG [9–11]. In addition to N-linked oligosaccharides, O-linked oligosaccharides have been determined in a human light chain [12].

The biological function of Fab-linked oligosaccharides still remains to be elucidated. The glycosylation of Fab fragments of IgG antibodies seems to be associated with several inflammatory diseases [13]. The presence of light-chain-associated carbohydrates has also been reported in diseases featuring tissue deposition of monoclonal light chains, such as primary amyloidosis and light-chain-deposition disease [6,14,15].

The primary object of the present study was to determine the structures of the Fab-linked oligosaccharides of a human monoclonal IgG. This polyspecific antibody was derived from a healthy donor and belongs therefore to the natural immunoglobulin repertoire. We report the complete structures of the major oligosaccharides of this human monoclonal IgG as determined by fluorophore-assisted carbohydrate electrophoresis (FACE®) and anion-exchange chromatography. Further, the influence of the oligosaccharides on antigen binding was tested in several immunoassays. A three-dimensional structure of the glycosylated variable (Fv) fragment was obtained by a two-step procedure. First, the structure of the Fv fragment was predicted using homology modelling, then one of the most prevalent oligosaccharides determined on the antibody was modelled *de novo* using an extended force field with CHARMm [16,17].

MATERIALS AND METHODS

Monoclonal antibody

The CBGA1-secreting human–human–mouse heterohybridoma was obtained from the peripheral blood lymphocytes of a healthy donor as described previously [18]. N-Deglycosylated CBGA1 was obtained by culturing the hybridoma cells (10^6 cells/ml) in 500 ml roller bottles containing medium with 2 μg of tunica-

Abbreviations used: ANTS, 8-aminonaphthalene-1,3,6,-trisulphonate; CDR, complementarity determining region; Fab, fragment of antigen binding; FACE®, fluorophore-assisted carbohydrate electrophoresis; Fc, crystallizing fragment; Fv, variable fragment; HPAEC/PAD, high-pH anion-exchange chromatography with pulsed amperometric detection; HRP, horseradish peroxidase; V_H, variable region of the heavy chain; V_L, variable region of the light chain; ds, double-stranded.

[1] To whom correspondence should be addressed at: Department of Dermatology, Medical School (Charité), Humboldt University Berlin, Schumannstr. 20/21, D-10117 Berlin, Germany.

[2] Present address: Department of Clinical Immunology and Transfusion Medicine, University of Leipzig, Delitzscher Str. 141, D-04129 Leipzig, Germany.

mycin/ml (Sigma, St. Louis, MO, U.S.A.) at 37 °C for 4 h. Then, the cells were centrifuged (200 ***g***) and resuspended in 500 ml of fresh medium containing 2 μg of tunicamycin/ml. The cells were cultured at 37 °C for 3 days, and then the supernatant was harvested. The glycosylated and N-deglycosylated antibodies were purified by affinity chromatography on a Protein A–Sepharose column (Pharmacia, Uppsala, Sweden). Fab and crystallizing (Fc) fragments were prepared by papain protein cleavage. The fragments were separated from each other on a Protein A–Sepharose column [18].

SDS/PAGE and immunoblots

SDS/PAGE and protein transfer on to nitrocellulose were conducted as described previously [18]. The filters were blocked with PBS/0.1 % Tween 20, incubated with 1 μg/ml horseradish peroxidase (HRP)-labelled anti-[human heavy-chain (γ)] antibody and alkaline phosphatase-labelled anti-[human light-chain (λ)] antibody for 1 h. Double staining of γ- and λ-chains was performed following the procedures given previously [18].

Antigen-specific ELISA

The antigen binding properties of the CBGA1 were characterized using various ELISA systems. Microtitre plates were coated either with 10 μg/ml double-stranded (ds) DNA from calf thymus, or with angiotensin III (Sigma) in 0.1 M carbonate buffer (pH 9.5), or with diphtheria toxoid or tetanus toxoid (Behring Werke, Marburg, Germany) in PBS (1:5000). Coating was completed overnight in all cases. The microtitre plates were washed three times with PBS/0.05 % Tween 20, incubated with 50 μl of supernatant or purified antibody at ambient temperature for 90 min, and washed again. Then, the microtitre plates were incubated with HRP-labelled anti-human λ-chain antibody (MEDAC, Hamburg, Germany) for 90 min, and washed. The colour reaction was developed with H_2O_2 and *o*-phenylendiamine in the dark. Another human IgG1-λ antibody (STL-1, specific for staphylolysin) was used as a negative control.

Whole-bacterial-cell ELISA

Microtitre plates were coated with 200 μl of an inactivated bacteria suspension in PBS containing 0.001 % NaN_3 ($D = 1.6$, measured at 660 nm) at 37 °C for 3 h. The bacteria strains used were *Pseudomonas aeruginosa* PA C7-67, *Escherichia coli* O1 Z 204, *E. coli* O6 Z 133, *E. coli* 205 (O18), *Klebsiella* C7-51 and *P. aeruginosa* PA 220. The plates were washed with PBS/0.05 % Tween 20 and incubated with purified antibody at various concentrations at 37 °C for 90 min. The Gram-positive bacterium *Staphylococcus aureus* served as a negative control antigen. Bound antibody was detected by HRP-labelled anti-(human γ-chain) antibody.

Cloning and sequencing of heavy- and light-chain variable-region genes

Total RNA was prepared from hybridoma cells following standard protocols [19]. For first-strand cDNA synthesis, total RNA (5 μg) was annealed to a random hexamer nucleotide mix (Boehringer Mannheim GmbH, Mannheim, Germany) and extended using the AMV (avian myeloblastosis virus) reverse-transcriptase kit (Gibco BRL, Gaithersburg, MD, U.S.A.). The gene region coding for the immunoglobulin variable region of the heavy chain (V_H) was amplified using primer pairs with the 5′-framework 1 region (5′-CAGGTGCAGCTGCAGGAGTC-TGG-3′) and a joining region of the heavy chain stretch [5′-CTTGGTGGA(AG)GAGACGGTGACC-3′] [20]. The gene coding region for the immunoglobulin variable region of the light chain (V_L) was amplified using primer pairs with 5′-framework 1 region (5′-TCSTATCAGCTGACKCARCCNCC-CTC-3′) and a Jλ-stretch (5′-ACCTAAGATCTTGACCTTGG-TCCCAGTTCCGAA-3′) [21]. PCR was carried out in a thermal cycler running 35 cycles (60 s at 96 °C, 60 s at 50 °C, 60 s at 72 °C). Finally, after 35 cycles, the reaction mixtures were incubated at 72 °C for 10 min to ensure full extension of all PCR products. Three purified fragments of independent cDNA PCR reactions were cloned into pUC 18 and sequenced from multiple clones in both directions [22].

Monosaccharide composition analysis by high-pH anion-exchange chromatography with pulsed amperometric detection (HPAEC/PAD)

Aliquots of the CBGA1 Fab fragment were treated with 2 M trifluoroacetic acid at 100 °C for 4 h to release all monosaccharides. Then the trifluoroacetic acid was removed by drying the sample in a centrifugal vacuum evaporator. The dried sample was dissolved in water, and a volume containing 0.5–2 nmol of monosaccharides was injected on to a CarboPac PA-1 column (4.9 × 250 mm). Separation of the monosaccharides was carried out at ambient temperature on a Dionex Bio-LC system (Dionex, Sunnyvale, CA, U.S.A.). The column had been pre-equilibrated in 10 mM sodium hydroxide. The sample was eluted with 16 mM sodium hydroxide. The flow rate was 1 ml/min. The column was calibrated with an equimolar mixture containing 0.5 nmol each of galactose, fucose, mannose, glucose, *N*-acetylglucosamine and *N*-acetylgalactosamine.

Desialylation of the CBGA1 Fab fragment was carried out under mild acidic conditions. Acetic acid was added to aliquots of the CBGA1 Fab fragment to a final concentration of 2 M. The sample was incubated at 80 °C for 3 h and then dried in a centrifugal vacuum evaporator, and dissolved in water. A CarboPac PA-1 column was pre-equilibrated in 100 mM sodium hydroxide and 100 mM sodium acetate. The samples were eluted with 100 mM sodium hydroxide and 150 mM sodium acetate over 30 min. The column was calibrated with an equimolar mixture containing 0.5 nmol each of *N*-acetylneuraminic acid and *N*-glycolylneuraminic acid.

Treatment of the antibody with *endo*glycosidases

Before *endo*glycosidase treatment the Fab fragment of the antibody was reduced and S-carboxymethylated. The sample was dried in a centrifugal vacuum evaporator and resuspended in 0.05 M ammonium bicarbonate buffer, pH 7.8. *N*-Glycosidase F (2 m-units; EC 3.5.1.52; Genzyme, Cambridge, MA, U.S.A.) was added, and the sample was incubated at 37 °C for 16 h. For treatment with *endo*glycosidase H (EC 3.2.1.96; Boehringer Mannheim GmbH), the sample was diluted in 0.1 M sodium phosphate, pH 5.5, and incubated with 2.5 m-units of *endo*glycosidase H at 37 °C for 16 h. Carbohydrates were isolated from the protein by precipitation with ethanol. The supernatant, which contained the carbohydrates, was dried to a translucent pellet.

FACE®

Following the release of the oligosaccharides from the Fab fragment, the mixture of oligosaccharides was labelled with 8-aminonaphthalene-1,3,6,-trisulphonate (ANTS) using the FACE® N-linked oligosaccharide profiling kit. The derivatized

oligosaccharides were separated on an oligosaccharide-profiling gel (Glyko, Novato, CA, U.S.A.). Samples were electrophoresed in 0.5-mm-thick gels with 15 mA at 4–8 °C for 90 min. Imaging of the gel was performed using the FACE® imaging system. Single oligosaccharide bands were purified from a preparative gel as previously described [23].

Sequencing of N-linked oligosaccharides by FACE®

Purified, labelled oligosaccharides (50–100 pmol) were diluted in 0.05 M sodium phosphate buffer, pH 6.0, and treated with several *exo*glycosidase combinations. *Exo*glycosidases (2 μl each) were added to each sample. The *exo*glycosidases used were: sialidase from *Arthrobacter ureafaciens* (EC 3.2.1.18), which releases both α-linked NeuAc and *N*-glycolylneuraminic acid; β-galactosidase from *Diplococcus pneumoniae* (EC 3.2.1.23), which releases β(1,4)-linked galactose; β-*N*-acetylhexosaminidase from *Canavalia ensiformis* (EC 3.2.1.30), which releases β-GalNAc and β-GlcNAc; and α-mannosidase from *Canavalia ensiformis* (EC 3.2.1.24), which releases α-linked Man (Glyko). The *exo*glycosidase combinations were: reaction 1, no enzyme; reaction 2, sialidase; reaction 3, sialidase and β-galactosidase; reaction 4, sialidase, β-galactosidase and β-*N*-acetylhexosaminidase; reaction 5, sialidase, β-galactosidase, β-*N*-acetylhexosaminidase and α-mannosidase. The samples were incubated at 37 °C for 12–16 h, dried in a centrifugal vacuum evaporator, resuspended in loading buffer (Glyko) and separated by FACE®. The migration pattern and the known specificity of the *exo*glycosidases combined with the data from the monosaccharide composition analysis allowed the oligosaccharide sequence to be determined. A mixture of glucose polymers served as a standard.

Computer-assisted modelling

All calculations were performed on a Silicon Graphics workstation. The model of the Fv fragment was created by homology modelling. Alignment of the sequences was done for the light and heavy chains separately with the Needleman and Wunch algorithm [24] using the Dayhoff matrix [25] as implemented in QUANTA (MSI Inc., San Diego, CA, U.S.A.). The chains were minimized separately and then combined to reveal the complete Fv fragment using CHARMm [16]. One of the predominant oligosaccharides, the tetra-antennary oligosaccharide, was chosen for modelling of the carbohydrate part. Its sequence is shown in Table 2 (see below). The carbohydrate part was modelled by generating the core and the four antennae as separate chains and then combined to form the tetra-antennary structure. Subsequently, the solvated and glycosylated Fv fragment was minimized with CHARMm using an extended force field (CHEAT95) [17].

Modelling of the light chain of CBGA1

The sequence of V_L was aligned to those of the PDB database (version released April 1995) [26]. The human monoclonal antibody Hil (pdb code: 8fab; F. A. Saul and R. J. Poljak, unpublished work), with an amino acid sequence identity of 65.7%, served as structural basis for the light chain. Positions 1 (tyrosine) and 7 (leucine) were defined by regularization with CHARMm. Hypervariable loops were searched for by using a loop database that is part of QUANTA. The loops were also taken from the structure of Hil. Disulphide bonds were created by QUANTA. Then the polypeptide chain was energy minimized to a local energy minimum.

Modelling of the heavy chain of CBGA1

Modelling of the heavy chain was performed similar to that of the V_L region. The human monoclonal antibody fragment KOL (pdb code: 2ig2) [27] served as the basis for modelling, having a 65% amino acid sequence identity. CDR1 and CDR2 (where CDR is complementarity determining region) were taken from the structure of KOL, whereas CDR3 was taken from triosephosphate isomerase (pdb code: 1ypi) [28]. The undefined co-ordinates of the residue 113 (tyrosine) were set up by CHARMm regularization. After setting up the disulphide bonds, the chain was energy minimized to a local minimum.

Both chains were combined by a least-squares fit on to the Fv fragment of antibody 3D6 (pdb code: 1dfl) [29], and the resulting crude model again minimized to a local energy minimum.

Modelling of the carbohydrate chains

The model of the tetra-sialylated tetra-antennary oligosaccharide was generated in QUANTA, using the module 'sequence builder' for each chain separately. The chains were then combined to one molecule, avoiding physically unrealistic steric clashes by rotating ϕ and ψ angles manually. The resulting structure was minimized with CHARMm using the CHEAT95 force field [17]. The carbohydrate chain was bound to the Fv fragment via Asn-75 of the heavy chain. The resulting model was first minimized *in vacuo*. Then the glycosylated Fv fragment was solvated by surrounding every residue with an 8 Å sphere of water (TIP3P model) [30] and removing overlapping water molecules. The solvated molecule was minimized first with the protein–carbohydrate moiety fixed to relax the water, and then with all atoms free. Due to the large requirements of computer resources of the last minimization, this calculation was performed on a Cray Y-MP at the Zuse-Zentrum, Berlin, Germany.

RESULTS

Sequences of V_H and V_L

The gene of V_H belongs to the V_HIII gene family and the gene of V_L belongs to the $V_{L\lambda}$3 gene family, as deduced from cDNA sequence analysis [31]. The variable region of the heavy chain has a potential N-glycosylation sequence at position Asn 75 (Asn-

CBGA1 V_L region

```
1   YELVQPLSVS VALGQTAKIT CGGNNIGSKN
31  VHWYQQQTGQ APVLVIYRDS NRPSGIPERF
61  SGSNSGNTAT LTISRAQAGD EADYVCQVWD
91  SSTVVFGGGT KLTVLG
```

CBGA1 V_H region

```
1   EVQLVESGGG LVQPGGSLRL GCAASGFTFR
31  TYSMHWVRQA PGKGLEWVSY ITSGSDILYY
61  ADSVKGRFTI SRDNANNSLC LQMNSLRDED
91  TAVYFCARDG VVETGTYYYY YYMDVWGQGT
121 TVTVSS
```

Figure 1 Amino acid sequences of the V_H and V_L genes of the CBGA1 antibody

The sequences are shown using one-letter codes. The CDRs are printed in bold. The potential N-glycosylation site in the framework III region of the heavy chain is underlined and italic.

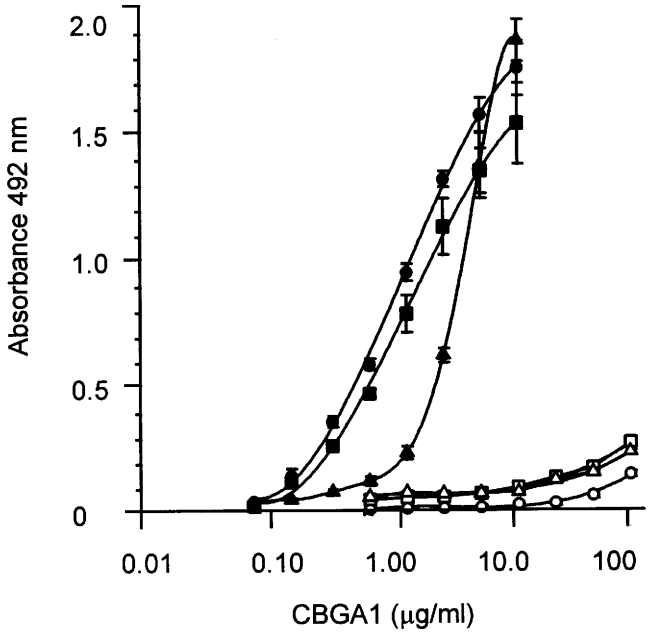

Figure 2 Antigen-binding activity of the CBGA1 antibody in a sandwich immunoassay

Antigen binding of untreated CBGA1 antibody (closed symbols) and by tunicamycin N-deglycosylated CBGA1 (open symbols) was assessed using a sandwich immunoassay. Antigens immobilized on to microtitre plates were: tetanus toxoid (●,○); diphtheria toxoid (■,□); and dsDNA (▲,△).

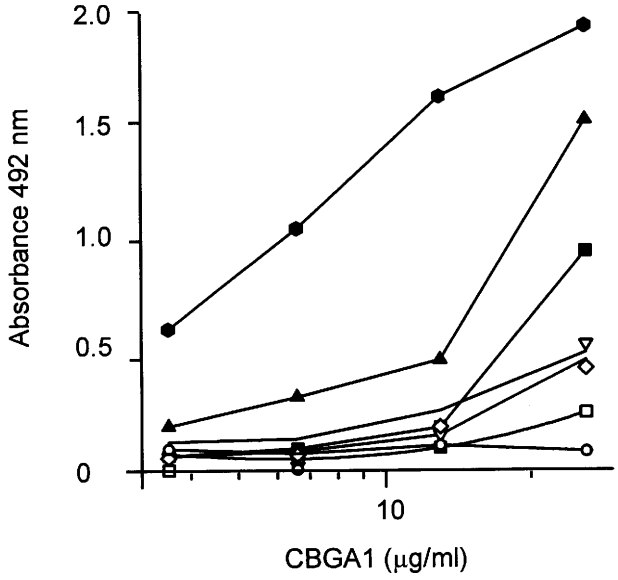

Figure 3 Antigen-binding activity of the CBGA1 antibody in a whole-bacteria ELISA

Dose-dependent binding of the CBGA1 to various bacteria strains immobilized on to microtitre plates was assessed in a whole-bacteria ELISA. ○, *S. aureus*; ⬣, *P. aeruginosa* PA C7–67; ▲, *E. coli* O1 Z 204; ■, *E. coli* O6 Z 133; ◇, *E. coli* 205 (O18); ▽, *Klebsiella* C7–51; □, *P. aeruginosa* PA 220.

Asn-Ser) which is located in the framework region III. The light chain does not have any potential N-glycosylation sequence (Asn-X-Ser/Thr; Figure 1). An aberrant cysteine was detected in the V_H region at position 79.

Antibody purification and fragmentation

An electrophoretically homogeneous antibody was obtained after purification using a Protein A column. The monoclonal antibody secreted by the tunicamycin-treated cells showed a shift of the γ-chain to a lower molecular mass in SDS/PAGE under reducing conditions. However, suppression of the glycosylation of the CBGA1 antibody by treatment with the N-glycosylation inhibitor tunicamycin was not complete. A small amount of glycosylated antibody remained in the supernatant. The treatment of the cells with higher concentrations of tunicamycin resulted in very low viability of the hybridoma cells and a marked decrease in antibody secretion. The λ-chain remained unchanged. Thus, all N-linked oligosaccharides appear to be located on the heavy chain of CBGA1, as predicted by amino acid sequence analysis.

Characterization of antigen binding

The antigen-binding pattern of the CBGA1 antibody was characterized using different types of immunoassay. CBGA1 reacted with various proteins, peptides and DNA in solid-phase sandwich immunoassays. Strong antigen binding to tetanus toxoid, diphtheria toxoid and dsDNA was observed. In an inhibition assay a K_d of 1.4×10^{-7} mol/l was determined for tetanus toxoid. A lower antigen-binding affinity was determined for the peptide angiotensin III. No binding was observed to the non-coated microtitre plates. The ability of the N-deglycosylated CBGA1 to bind to tetanus toxoid, diphtheria toxoid and dsDNA was reduced more than 100-fold (Figure 2).

In a whole-bacteria ELISA a strong binding to *P. aeruginosa* PA C7-67, *E. coli* O1 Z 204 and *E. coli* O6 Z 133 was observed. Less effective binding was observed to *E. coli* 205 (O18) and *Klebsiella* C7-51. The CBGA1 antibody bound neither to *P. aeruginosa* PA 20 nor to the Gram-positive bacterium *S. aureus* (Figure 3). The human monoclonal IgG STL-1 antibody (specific for staphylolysin), which was used as a negative control IgG in all tests, did not bind to any of these antigens.

Table 1 Monosaccharide composition of the CBGA1 Fab fragment analysed by HPAEC/PAD

Monosaccharide	Amount (μg/100 μg of sample)	Mol% of total carbohydrates in CBGA1
Fucose	0.53	7.1
Galactose	1.36	16.8
N-Acetylglucosamine	3.32	32.2
N-Acetylgalactosamine	0.05	0.45
Mannose	1.96	23.9
N-Acetylneuraminic acid	0.18	1.2
N-Glycolylneuraminic acid	2.83	18.2

Monosaccharide composition analysis

The monosaccharide composition (Table 1) of the CBGA1 Fab fragment was determined by HPAEC/PAD. The carbohydrate residues accounted for 10.2% of the mass of the CBGA1 Fab

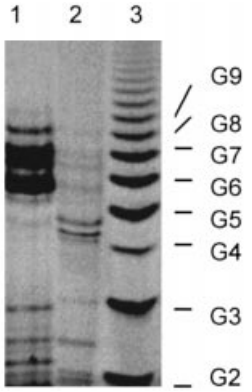

Figure 4 Oligosaccharide profile of the oligosaccharides derived from the CBGA1 Fab fragment using FACE®

Lane 1, oligosaccharides released by treatment with *N*-glycosidase F; lane 2, oligosaccharides released by treatment with *endo* glycosidase H; lane 3, oligosaccharide ladder standard (glucose polymers).

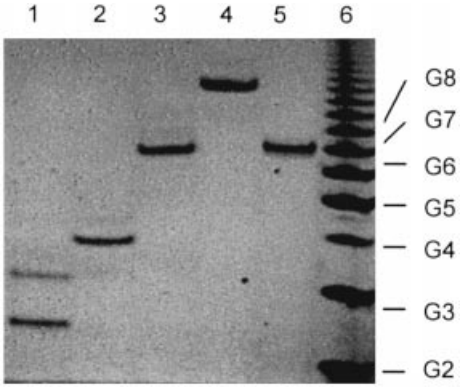

Figure 5 Sequence analysis of a tetra-sialylated tetra-antennary complex-type oligosaccharide derived from the CBGA1 Fab fragment by sequential *exo*glycosidase treatment using FACE®

Lane 1, purified oligosaccharide treated with sialidase, β-galactosidase, β-*N*-acetylhexosaminidase and α-mannosidase; lane 2, purified oligosaccharide treated with sialidase, β-galactosidase and β-*N*-acetylhexosaminidase; lane 3, purified oligosaccharide treated with sialidase and β-galactosidase; lane 4, purified oligosaccharide treated with sialidase; lane 5, purified oligosaccharide; lane 6, oligosaccharide ladder standard (glucose polymers).

Table 2 Most prevalent oligosaccharide structures present on the CBGA1 Fab fragment

The most prevalent oligosaccharide structures present on the *N*-glycosylation site of the CBGA1 Fab fragment were determined using sequential *exo*glycosidase treatment and FACE. Values are calculated as the percentage of oligosaccharide present in the oligosaccharide pool.

Oligosaccharide	% oligosaccharide of the oligosaccharide pool
NeuGcα(2,6/3)Galβ(1,4)GlcNAcβ(1,2)Manα(1,6) NeuGcα(2,6/3)Galβ(1,4)GlcNAcβ(1,2)Manα(1,3) Manβ(1,4)GlcNAcβ(1,4)GlcNAc-Asn α(1,6)Fuc	42.4
NeuGcα(2,6/3)Galβ(1,4)GlcNAcβ(1,4) NeuGcα(2,6/3)Galβ(1,4)GlcNAcβ(1,2)Manα(1,6) NeuGcα(2,6/3)Galβ(1,4)GlcNAcβ(1,2)Manα(1,3) NeuGcα(2,6/3)Galβ(1,4)GlcNAcβ(1,4) Manβ(1,4)GlcNAcβ(1,4)GlcNAc-Asn α(1,6)Fuc	21.5
NeuGcα(2,6/3)-[Galβ(1,4)GlcNAcβ(1,2)Manα(1,6) Galβ(1,4)GlcNAcβ(1,2)Manα(1,3)] Manβ(1,4)GlcNAcβ(1,4)GlcNAc-Asn α(1,6)Fuc	18.8
Galβ(1,4)GlcNAcβ(1,2)Manα(1,6) Galβ(1,4)GlcNAcβ(1,2)Manα(1,3) Manβ(1,4)GlcNAcβ(1,4)GlcNAc-Asn α(1,6)Fuc	7.6
NeuGcα(2,6/3)Galβ(1,4)GlcNAcβ(1,2)-[Manα(1,6) Manα(1,3)] Manβ(1,4)GlcNAcβ(1,4)GlcNAc-Asn α(1,6)Fuc	2.1
NeuGcα(2,6/3)Galβ(1,4)GlcNAcβ(1,2)-[Manα(1,6) Manα(1,3)] Manβ(1,4)GlcNAcβ(1,4)GlcNAc-Asn	1.5

fragment. The high amount of sialic acids (18.2 mol%) indicates that most of the oligosaccharides carried at least one neuraminic acid residue. The type of neuraminic acid was also analysed by HPAEC/PAD, after mild acid treatment of the CBGA1 Fab fragment. *N*-Acetylneuraminic acid and *N*-glycolylneuraminic acid were found to be present in a ratio of 6:94. A small amount of *N*-acetylgalactosamine was also released from the Fab fragment, suggesting that the CBGA1 antibody contains O-linked oligosaccharides.

Characterization of the N-linked oligosaccharides

The N-linked oligosaccharides of the CBGA1 Fab fragment were released using *endo*glycosidases, labelled with ANTS and analysed using FACE®.

A very heterogeneous glycosylation pattern was found in the CBGA1 Fab fragment. Some oligosaccharides showed very similar electrophoretic mobilities and migrated close to each other in the gel (e.g. certain high-mannose-type glycans and certain complex-type sialylated glycans). Therefore, hybrid- and high-mannose-type oligosaccharides were initially released with *endo*glycosidase H, separated from the Fab fragment, and analysed (Figure 4, lane 2). In a second step, all remaining oligosaccharides were released from the Fab fragment with *N*-glycosidase F (Figure 4, lane 1). Seven complex-type oligosaccharides and six hybrid/high-mannose-type oligosaccharides were detected (Figure 4)

Sequence analysis of the predominant oligosaccharides of the CBGA1 Fab fragment

ANTS-labelled oligosaccharides were separated on a preparative electrophoresis gel, the most prevalent oligosaccharide bands were excised and the oligosaccharides were extracted from the gel slices. Of the oligosaccharide pool of the CBGA1 Fab fragment (two predominant oligosaccharides released by *endo*glycosidase H, and four predominant complex-type oligosaccharides released by N-glycosidase F), 93% were extracted and purified for sequencing. The remaining oligosaccharides (6.7% of the total N-linked oligosaccharide pool) were present in insufficient quantities for sequencing. The isolated oligosaccharides were analysed by a sequential addition of highly specific *exo*glycosidases to the ANTS-labelled oligosaccharides, which were subsequently separ-

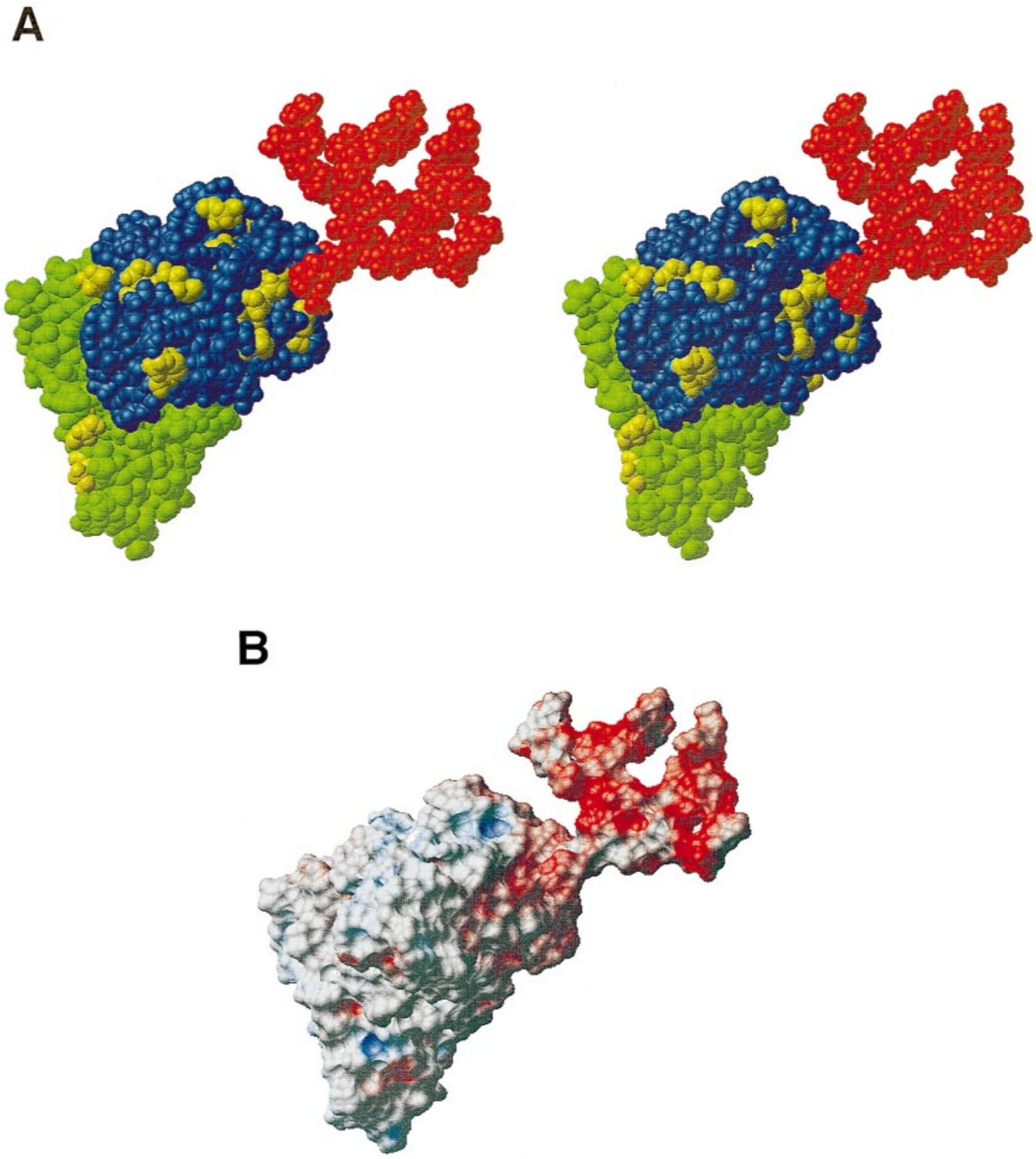

Figure 6 Three-dimensional structure of the glycosylated Fv fragment of antibody CBGA1

(**A**) Stereo view of the three-dimensional structure of the glycosylated Fv fragment of antibody CBGA1 as a Corey–Pauling–Koltun model. The light chain is coloured green, the heavy chain is blue, and the tetra-sialylated tetra-antennary complex oligosaccharide is red. Serines on the surface, i.e. possible O-glycosylation sites, are in yellow. (**B**) Charge distribution in the glycosylated Fv fragment of CBGA1. The colour range is from blue (negative) to red (positive). Figures were created using ICM [34].

Table 3 Hydrogen bonds in the three-dimensional model of the glycosylated Fv fragment of CBGA1

For the antibody, only inter-segment hydrogen bonds are shown. Chain identifiers, shown in bold: L, light antibody chain; H, heavy antibody chain; C, glycosylation core segment; 1, 2, 3 or 4, sugar chains 1, 2, 3 or 4, respectively. NeuGc, *N*-glycolylneuraminic acid.

	Donor		Acceptor					
Residue	Atom 1	Atom 2	Atom 3	Atom 4	Residue	∠123 (°)	d23 (Å)	∠234 (°)
Trp **L**33	N	H	Oη	Cζ	Tyr **H**111	154.8	1.87	127.5
Tyr **L**47	Oh	Hh	O	C	Tyr **H**108	163.1	1.88	109.8
Leu **H**45	N	H	Oδ2	Cγ	Asp **L**83	171.9	2.27	116.4
Trp **H**47	Nϵ1	Hϵ1	O	C	Val **L**94	140.7	2.22	136.0
Tyr **H**109	Oh	Hh	O	C	Tyr **L**47	176.7	1.76	174.7
Tyr **H**110	N	H	Nϵ2	Cδ2	His **L**32	144.4	2.26	122.2
Tyr **H**110	Oη	Hη	O	C	Ser **L**92	134.0	2.44	108.2
Tyr **H**111	Oη	Hη	O	C	Trp **L**33	109.6	2.39	117.4
Tyr **H**111	Oη	Hη	O	C	Leu **L**44	155.2	1.77	122.4
GlcNAc **C**2	O3	HO3	O7	C7	GlcNAc **C**2	152.3	1.73	115.9
GlcNAc **C**3	O3	HO3	O5	C1	GlcNAc **C**2	138.7	2.00	98.1
Gal **1** 2	O6	HO6	O5	C1	Gal **1** 2	100.8	2.27	141.4
Gal **1** 2	O6	HO6	O3	C3	GlcNAc **1** 3	174.9	1.83	127.8
GlcNAc **1** 3	N2	HN	O7	C7	GlcNAc **C**2	159.8	1.86	119.0
GlcNAc **1** 3	O3	HO3	O5	C1	GAL **1** 2	119.8	1.89	107.4
GlcNAc **1** 3	O6	HO6	O5	C1	GlcNAc **1** 3	105.5	1.99	150.9
Gal **2** 2	O3	HO3	O9	C9	NeuGc **1** 1	130.2	2.40	110.4
GlcNAc **2** 3	O3	HO3	O7	C7	GlcNAc **2** 3	136.4	1.83	101.1
GlcNAc **2** 3	O6	HO6	O6	C6	GlcNAc **1** 3	143.4	1.77	121.5
GlcNAc **2** 3	O6	HO6	O5	C1	GlcNAc **2** 3	97.6	2.33	157.7
Gal **3** 2	O4	HO4	O3	C2	Gal **3** 1	104.8	2.44	129.1
Gal **3** 2	O6	HO6	O5	C1	Gal **3** 2	104.9	2.23	144.4
GlcNAc **3** 3	O3	HO3	O4	C1	GlcNAc **3** 2	108.0	2.36	111.9
GlcNAc **3** 3	O6	HO6	O5	C1	GlcNAc **3** 3	110.2	2.33	137.0
NeuGc **4** 1	O7	HO7	O6	C2	NeuGc **4** 1	108.0	2.26	149.0
NeuGc **4** 1	O8	HO8	O1	C1	NeuGc **4** 1	173.3	2.48	129.9
Gal **4** 2	O3	HO3	O5A	C5A	NeuGc **3** 1	148.1	1.92	146.4
GlcNAc **4** 3	N2	HN	O3	C3	Man **4** 4	148.3	2.25	105.3
GlcNAc **4** 3	O3	HO3	O7	C7	GlcNAc **4** 3	157.0	1.81	98.5
GlcNAc **4** 3	O6	HO6	O6	C6	GlcNAc **3** 3	154.1	1.78	141.7
Man **4** 4	O3	HO3	O4	C1	Man **4** 3	105.4	2.43	114.1
Man **4** 4	O6	HO6	O5	C1	Man **4** 4	105.5	1.97	151.3

ated using FACE®. The release of particular monosaccharide residues at the exposed non-reducing end was deduced from the increased mobility of the remaining ANTS-labelled oligosaccharide in the gel relative to standards.

The mobilities of three of the four complex-type oligosaccharides were decreased by sialidase treatment. Their mobilities decreased by a value equivalent to the removal of one, two or even four sialic acids, respectively. Therefore, the CBGA1 Fab fragment possesses mono-, di- and tetra-sialylated complex-type oligosaccharides. The predominant structure (42.4 %) is a di-sialylated bi-antennary complex oligosaccharide. Furthermore, the Fab fragment possesses almost equal amounts (18.8 and 21.5 % of the total oligosaccharide pool) of a mono-sialylated and a tetra-sialylated complex oligosaccharide respectively. A non-sialylated di-galactosylated complex-type oligosaccharide was determined to be present in minor amounts (7.6 % of the whole oligosaccharide pool). All complex oligosaccharides contain a fucosylated pentasaccharide core structure. The complete structures of all sequenced oligosaccharides are given in Table 2 and the sequence analysis of a tetra-sialylated tetra-antennary complex oligosaccharide is shown in Figure 5.

The electrophoretic mobilities of the two oligosaccharides isolated from the *endo*glycosidase H digest also decreased after treatment with sialidase by an amount equivalent to the removal of one sialic acid. These two oligosaccharides differ from each other only in one fucosyl residue attached to their pentasaccharide core structure. No high-mannose-type oligosaccharides were detected in the CBGA1 Fab fragment.

Three-dimensional structure of the glycosylated Fv fragment

The tetra-sialylated tetra-antennary oligosacharide was chosen for the modelling experiment because it is one of the predominant oligosaccharides. Further, one may expect the strongest influence of this oligosaccharide on the antigen-binding site of this antibody because of its large size and charge. The tetra-sialylated tetra-antennary complex oligosaccharide is 15.5 % of the whole volume of the molecule of 31749 Å^3, calculated by program MSB [32]. It extends away from the antibody fragment, as can be seen in red in Figure 6(A). The fucose residue bends towards the glycosylic bond of Asn-75 to the glycosylation part. Hydrogen bonds of the glycosylation part and between antibody light and heavy chains are shown in Table 3. Dihedral angles of the glycosylation part are shown in Table 4. The glycosylation part occupies 27.3 % of the solvent-accessible surface of 13363 Å^2 (calculated with a probe radius of 1.4 Å) [33]. The electrostatic energy of the molecule was calculated using program ICM [34,35] by solving the linearized Poisson–Boltzman equation. The electrostatic free energy amounted to -9856 kcal/mol (1 cal $\equiv$ 4.184 J), and the charge of the molecule to -5.6 asu. The charge distribution is

Table 4 Dihedral angles of the glycosylation moiety of CBGA1

Chain identifiers, shown in bold: C, glycosylation core segment; 1, 2, 3 or 4, sugar chains 1, 2, 3 or 4, respectively.

Linkage	ϕ	ψ	ω
Core			
Man(**C**1)β1–4GlcNAc(**C**2)	−20.6	−4.2	
GlcNAc(**C**2)β1–4GlcNAc(**C**3)	122.2	−48.4	
GlcNAc(**C**3)β6–1aFuc(**C**4)	−90.8	−175.2	−45.4
Man(**2** 4)α1–6Man(**C**1)	32.0	−49.8	41.1
Man(**4** 4)α1–3Man(**C**1)	−26.7	−23.3	
Chain 1			
NeuGc(**1** 1)α2–3Gal(**1** 2)	−112.7	−8.3	
Gal(**1** 2)β1–4GlcNAc(**1** 3)	50.7	9.1	
GlcNAc(**1** 3)β1–4Man(**2** 4)	151.1	−113.9	−91.6
Chain 2			
NeuGc(**2** 1)α2–3Gal(**2** 2)	140.8	167.3	−43.9
Gal(**2** 2)β1–4GlcNAc(**2** 3)	30.1	−3.0	
GlcNAc(**2** 3)β1–2Man(**2** 4)	65.6	163.1	
Chain 3			
NeuGc(**3** 1)α2–3Gal(**3** 2)	−155.6	−35.6	
Gal(**3** 2)β1–4GlcNAc(**3** 3)	43.4	40.3	
GlcNAc(**3** 3)β1–4Man(**4** 4)	61.0	33.9	
Chain 4			
NeuGc(**4** 1)α2–3Gal(**4** 2)	−138.6	−156.3	−85.8
Gal(**4** 2)β1–4GlcNAc(**4** 3)	49.5	−23.2	
GlcNAc(**4** 3)β1–2Man(**4** 4)	−65.8	−71.5	

depicted in Figure 6(B). Serines, which are potential O-glycosylation sites, are coloured yellow in Figure 6(A).

DISCUSSION

We have described the structures of the most abundant oligosaccharides present on the Fab fragment of the human monoclonal IgG CBGA1 and the possible influence of the oligosaccharides on its antigen binding. The antibody was derived from a healthy donor and reacts with various foreign and/or self antigens.

One potential N-glycosylation site was found in the Fv fragment of the CBGA1 antibody by sequence analysis of its variable regions. This N-glycosylation site is located in the V_H region at position Asn-75. IgG antibodies are normally not glycosylated in their Fab fragments. There are a few reports of Fab-glycosylated antibodies, mostly found in myeloma patients [4,36]. There seem to be no general rules for the occurrence of potential N-glycosylation sites in the Fv fragment. However, there seem to be some regions in the Fv fragments that more often contain the N-glycosylation consensus sequence (Asn-Xaa-Ser/Thr). These regions are CDR1 and CDR3 of the V_L region, and the framework III on position Asn-72 of the V_H region [15,31].

Only limited information is available regarding the precise structures of Fv-associated oligosaccharides. So far, all carbohydrates found in the variable regions of antibodies have been characterized as bi-antennary complex type. Most of these structures were found to be mono- or di-sialylated oligosaccharides and to contain a fucosylated pentasaccharide core structure [36,37]. Some antibodies also contain high-mannose-type and/or hybrid-type oligosaccharides in their variable regions [8,11]. The glycosylation site in the CBGA1 Fv fragment is occupied by up to 13 different oligosaccharides. Tetra-sialylated tetra-antennary-, di-sialylated bi-antennary- and mono-sialylated bi-antennary complex oligosaccharides predominate together with 82.7% the Fv-linked oligosaccharides of the CBGA1. This is the first report of a tetra-antennary complex oligosaccharide attached to the Fv fragment of a human monoclonal antibody.

About 19% of the monosaccharides of the CBGA1 Fab fragment are neuraminic acids, which is a much higher amount than is usually found in Fc-associated oligosaccharides [9]. Over 93% of all determined neuraminic acids in this antibody are *N*-glycolylneuraminic acids. Glycoproteins in adult humans do not normally contain any *N*-glycolylneuraminic acid, which has been considered as an oncofetal antigen [38]. However, there are reports of human monoclonal IgG and IgM expressing variable ratios of *N*-acetylneuraminic acid and *N*-glycolylneuraminic acid (ranging from 0 to 92% *N*-glycolylneuraminic acid) [39,40]. The presence of *N*-glycolylneuraminic acid in the antibody suggests a dominance of the mouse glycosylation machinery in the human–human–mouse heterohybridoma CBGA1. The antigenic properties of *N*-glycolylneuraminic acid in humans may stimulate an anti-*N*-glycolylneuraminic acid immune response dependent on the dosage if the antibody is used *in vivo* [41]. This immune response is likely to influence the *in vivo* effect of the antibody, thereby limiting its therapeutic value. Furthermore, terminal *N*-glycolylneuraminic acid on a recombinant protein also seems to be correlated with a more rapid removal of the molecule from the circulatory system [42]. The unusual mono- and oligo-saccharides (*N*-glycolylneuraminic acid and the tetra-antennary oligosaccharide), and the heterogeneity of the oligosaccharide pool, as determined for the CBGA1 antibody, suggest that the method of immortalization and the host cell line, as well as the culture conditions, may have an impact on both the biological activity and availability of antibodies produced for use *in vivo*.

N-Acetylgalactosamine was also found to be present in the CBGA1 antibody, as determined by monosaccharide composition analysis, although it is only present on about 6% of all CBGA1 molecules. The presence of GalNAc indicates the presence of O-linked oligosaccharides in the CBGA1. IgG antibodies do not normally contain O-linked oligosaccharides. However, the presence of an O-linked oligosaccharide was described for a light chain derived from a myeloma patient [12]. Further, other antibody isotypes such as IgA do normally contain O-linked oligosaccharides in their hinge region. The position of the attachment of the GalNAc to the polypeptide chain of the CBGA1 Fab fragment was not determined in this study.

The presence of a large bulky carbohydrate portion in the Fv region of this antibody prompted us to test its influence on the antigen-binding activity of the antibody. All Fv-glycosylated human monoclonal antibodies described in the literature are monospecific. They were derived from patients and had their origins from an antigen-driven high-affinity maturation process *in vivo* [43]. The CBGA1 antibody bound to several antigens of a different primary structure, such as tetanus toxoid, dsDNA and lipopolysaccharide from various bacteria strains. These data suggest that the CBGA1 antibody belongs to the group of polyspecific antibodies described earlier [44,45]. Polyspecific antibodies display mostly low affinities for their self and/or foreign antigens [46,47]. The mechanism by which polyspecific antibodies bind to distinctly different antigens has not been clearly established and their biological function is currently under discussion. Considering the antigen spectrum of polyspecific antibodies, the polyspecificity of antibodies may serve in the first line of defence of the immune system against exogenous antigens, such as bacteria and toxins. These antibodies may also be useful in removing altered self or released intracellular components, such as DNA. In the evolutionary selection process for high-affinity monospecific antibodies, N-glycosylation sites in or close to the antigen-binding region seem to have been

disadvantageous, because glycosylation is an inherently complex post-translational process that can be influenced by a variety of factors (cell type, state of the cell, disease, culture conditions, etc.). However, for the low-affinity polyspecific antibodies the glycosylation may enhance their binding properties due to conformational changes or charge distribution. Most polyspecific antibodies described are IgMs, which are normally much more heavily glycosylated than IgGs.

The main aim of modelling the three-dimensional structure of the Fv fragment with carbohydrates attached to it was to determine the space requirements and charge distribution of a large Fv-attached oligosaccharide. The model of the three-dimensional structure was achieved in a two-step process. First, the Fv fragment was modelled by homology modelling, as described in the Materials and methods section, which is nowadays common practice. For the modelling of glycosylation, however, there is no such commonly accepted protocol. Therefore, the carbohydrate part was modelled *de novo*, using CHEAT95, an extended force field, based on the commonly known CHARMm force field. There is no known preference for a single conformation. NMR data suggest that there is an ensemble of various structures for the glycosylation part rather than one single structure [48–50]. Therefore, the modelled glycosylation part was energy-minimized in solvent. No Monte Carlo conformational searches could be done, because the appropriate force fields (e.g. ECEPP/3) are not parameterized for carbohydrates. For a more detailed description of the model, hydrogen bonds are given in Table 3 and dihedral angles of the glycosylation part in Table 4. As can be seen in Figure 6, the oligosaccharide portion linked to the CBGA1 Fv fragment points away from its antigen-binding site. Therefore, it probably does not directly influence the antigen binding activity of this antibody, but the glycosylation may alter the antigen-binding region by changing its conformation. Putative antigen-binding sites of the antibody may also be hidden by the variable-region-associated oligosaccharides. N-Deglycosylation of the CBGA1 antibody by cultivation of the hybridoma cells with tunicamycin resulted in a reduction or loss of antigen-binding activity for all tested antigens. Therefore, the CBGA1 antibody belongs to the group of antibodies with Fv-associated oligosaccharides that express a higher affinity for their antigens due to their Fv glycosylation. However, there are also antibodies in which the Fv-associated carbohydrates decrease their antigen-binding affinity [43]. In a third group of antibodies the presence or absence of variable-region-associated oligosaccharides does not affect the affinity or specificity of these antibodies [2,51]. Recently, it has been demonstrated that the carbohydrate structure of a light chain can be altered by supplementing the medium with more than 20 mM *N*-acetylglucosamine. The newly induced light-chain glycoform showed a 10-fold increased antibody affinity [11]. The possible influence of the variable-region glycosylation of antibodies on their affinity and specificity makes these oligosaccharides interesting targets to improve the diagnostic or therapeutic value of Fab-glycosylated monoclonal antibodies.

We wish to thank P. Siegel and B. Kersten for assistance in sequencing the antibody variable-region genes. The assistance of Th. Steinke (Zuse-Zentrum, Berlin, Germany) with using the Cray Computer is gratefully acknowledged. This work was supported in part by Deutsche Forschungsgemeinschaft grant LE 1000/1-1, EU-BioTech (BIO4-CT96-0129) and the Swedish Medical Research Council (no. 7461).

REFERENCES

1 Donadel, G., Calabro, A., Sigounas, G., Hascall, V. C., Notkins, A. L. and Harindranath, N. (1994) Glycobiology **4**, 491–496
2 Leung, S., Goldenberg, D. M., Dion, A. S., Pellegrini, M. C., Shevitz, J., Shih, L. B. and Hansen, H. J. (1995) Mol. Immunol. **32**, 1413–1427
3 Khurana, S., Raghunathan, V. and Salunke, D. M. (1997) Biochem. Biophys. Res. Commun. **234**, 465–469
4 Spiegelberg, H. L., Abel, C. A., Fishkin, B. G. and Grey, H. M. (1970) Biochemistry **9**, 4217–4223
5 Sox, H. C. and Hood, L. (1970) Proc. Natl. Acad. Sci. U.S.A. **66**, 975–982
6 Decourt, C., Cogne, M. and Rocca, A. (1996) Clin. Exp. Immunol. **106**, 357–361
7 Wallik, S. C., Kabat, E. A. and Morrison, S. L. (1988) J. Exp. Med. **168**, 1099–1109
8 Wright, A., Tao, M., Kabat, A. E. and Morrison, S. L. (1991) EMBO J. **10**, 2717–2723
9 Rademacher, T. W., Homans, S. W., Parekh, R. B. and Dwek, R. A. (1988) Biochem. Soc. Symp. **51**, 131–138
10 Savidou, G., Klein, M., Grey, A. A., Dorrington, K. J. and Carver, J. P. (1984) Biochemistry **23**, 3736–3740
11 Tachibana, H., Kim, Y. Y. and Shirahata, S. (1997) Cytotechnology **23**, 151–159
12 Chandrasekaran, E. V., Mendicino, A., Garver, F. A. and Mendicino, J. (1981) J. Biol. Chem. **256**, 1549–1555
13 Middaugh, C. R. and Litman, G. W. (1987) J. Biol. Chem. **262**, 3671–3673
14 Holm, E., Sletten, K. and Husby, G. (1986) Biochem. J. **239**, 545–552
15 Fykse, E. M., Sletten, K., Husby, G. and Cornwell, G. G. (1988) Biochem. J. **256**, 973–980
16 Brooks, B. R., Bruccoleri, R. E., Olafson, B. D., States, D. J., Swaminathan, S. and Karplus, M. (1983) J. Comput. Chem. **4**, 187–217
17 Kouwijzer, M. L. C. E. and Grootenhuis, P. D. J. (1995) J. Phys. Chem. **99**, 13426–13436
18 Leibiger, H., Hansen, A., Schoenherr, G., Seifert, M., Wüstner, D., Stigler, R. and Marx, U. (1995) Mol. Immunol. **32**, 595–602
19 Sambrook, J., Fritsch, E. and Maniatis, T. (1989) Molecular Cloning: A Laboratory Manual, vols. 1–3, Cold Spring Harbor Press, Cold Spring Harbor
20 Marks, J. D., Tristem, M., Karpas, A. and Winter, G. (1991) Eur. J. Immunol. **21**, 985–992
21 Songsviali, S., Bye, J. M., Marks, J. D. and Hughes-Jones, N. C. (1990) Eur. J. Immunol. **20**, 2661–2666
22 Sanger, F., Nicklen, S. and Coulson, A. R. (1977) Proc. Natl. Acad. Sci. U.S.A. **74**, 5463–5471
23 Leibiger, H., Kersten, B., Albersheim, P. and Darvill, A. (1998) Glycobiology **8**, 497–507
24 Needleman, S. B. and Wunch, C. D. (1970) J. Mol. Biol. **48**, 443–453
25 Dayhoff, M. O. (1978) Atlas of Protein Sequence and Structure, vol. 5, suppl. 3, Biomedical Research Foundation, Silver Spring
26 Bernstein, F. C., Koetzle, T. F., Williams, G. J. B., Meyer, Jr., E. F., Brice, M. D., Rodgers, J. R., Kennard, O., Shimanouchi, T. and Tasumi, M. (1977) J. Mol. Biol. **112**, 535–542
27 Kratzin, H. D, Palm, W., Stangel, M., Schmidt, W. E, Friedrich, J. and Hilschmann, N. (1989) Biol. Chem. Hoppe-Seyler **370**, 263–272
28 Lolis, E., Alber, T., Davenport, R. C., Rose, D., Hartman, F. C. and Petsko, G. A. (1990) Biochemistry **29**, 6609–6618
29 Min He, X., Rüker, F., Casale, E. and Carter, D. C. (1992) Proc. Natl. Acad. Sci. U.S.A. **89**, 7154–7158
30 Jorgensen, W. L. and Ibrahim, M. (1981) J. Am. Chem. Soc. **103**, 3976–3985
31 Kabat, E. A., Wu, T. T., Reid-Miller, M., Rerry, H. M. and Gottesmann, K. S. (1991) Sequences of Proteins of Immunological Interest, 5th edn., US Department of Health and Human Services, National Institutes of Health, Bethesda
32 Connolly, M. L. (1983) J. Appl. Crystallogr. **16**, 548–558
33 Lee, B. and Richards, F. M. (1971) J. Mol. Biol. **55**, 379–400
34 Abagyan, R., Totrov, M. and Kuznetsov, D. (1994) J. Comput. Chem. **15**, 488–506
35 Zauhar, R. J. and Morgan, R. S. (1985) J. Mol. Biol. **186**, 815–820
36 Kinoshita, N., Ohno, M., Nishiura, T., Fujii, S., Nishikawa, A., Kawakami, Y., Uozumi, N. and Taniguchi, N. (1991) Cancer Res. **51**, 5888–5892
37 Coco-Martin, J. M., Brunik, F., Van Der Velden De Groot, T. A. M. and Beuyvery, E. C. (1992) J. Immunol. Methods **155**, 241–248
38 Muchmore, E. A., Milewski, M., Varki, A. and Diaz, S. (1989) J. Biol. Chem. **264**, 20216–20223
39 Monica, T. J., Williams, S. B., Gochee, C. F. and Maiorella, B. L. (1995) Glycobiology **5**, 175–185
40 Tandai, M., Endo, T., Sasaki, S., Masuho, Y., Kochibe, N. and Kobata, A. (1991) Arch. Biochem. Biophys. **231**, 339–348
41 Noguchi, A., Mukuria, C. J., Suzuki, E. and Naiki, M. (1995) J. Biochem. (Tokyo) **117**, 59–62
42 Flesher, A. R., Marzowski, J., Wang, W. C. and Raff, H. V. (1995) Biotechnol. Bioeng. **46**, 399–407

43 Kato, M., Mochizuki, K., Hashizume, S., Tachibana, H., Shirahata, S. and Murakami, H. (1993) Hum. Antibodies Hybridomas **4**, 9–14
44 Rosenstein, R. W., Musson, R., Armstrong, M., Konigsberg, W. H. and Richards, F. (1972) Proc. Natl. Acad. Sci. U.S.A. **69**, 877–881
45 Avrameas, S. and Ternyck, T. (1993) Mol. Immunol. **30**, 1133–1142
46 Casali, P. and Notkins, A. L. (1989) Annu. Rev. Immunol. **7**, 513–525
47 Adib-Conouy, M., Avrameas, S. and Ternyck, T. (1993) Mol. Immunol. **30**, 119–127
48 Rutherford, T. J., Partridge, J., Weller, C. T. and Homans, S. W. (1993) Biochemistry **32**, 12715–12724
49 Rutherford, T. J. and Homans, S. W. (1994) Biochemistry **33**, 9606–9614
50 Rutherford, T. J., Neville, D. C. and Homans, S. W. (1995) Biochemistry **34**, 14131–14137
51 Sato, K., Ohtomo, T., Saito, H., Matsuura, T., Akimoto, T., Akamatsu, K. I., Koishihara, Y., Ohsugai, Y. and Tsuchiya, M. (1996) Hum. Antibodies Hybridomas **7**, 175–183

Received 5 August 1998/11 November 1998; accepted 4 December 1998